

# Bragg scattering of Cooper pairs in an ultra-cold Fermi gas

K. J. Challis,\* R. J. Ballagh, and C. W. Gardiner

*Jack Dodd Centre for Photonics and Ultra-Cold Atoms*

*Department of Physics, University of Otago, P.O. Box 56, Dunedin, New Zealand*

(Dated: October 19, 2019)

We present a theoretical treatment of Bragg scattering of a degenerate Fermi gas, based on the time-dependent Bogoliubov de Gennes equations. Numerical solutions show that, in addition to the expected single-particle Bragg scattering, correlated scattering of atom pairs occurs via a grating formed in the pair potential. The correlated-pair Bragg scattering has a sharp frequency threshold, beyond which the scattered pairs form a spherical shell in momentum space that is centered at half the usual Bragg momentum transfer. We develop an analytic model that explains key features of correlated-pair Bragg scattering.

PACS numbers: 03.75.Ss, 32.80.Cy

Bragg scattering provides a high precision spectroscopic technique that has been adapted from materials science to probe Bose-Einstein condensates [1, 2]. Signatures of condensate properties, such as thermal fluctuations [3], vortex flow [4], and solitary-wave motion [5, 6], are accessible due to the velocity selectivity of Bragg spectroscopy. It has been proposed [7, 8, 9, 10] that Bragg spectroscopy of an ultra-cold Fermi gas can provide insight into the Cooper paired regime, and the transition through a Feshbach resonance to molecule formation.

In this paper we develop Bragg spectroscopy as a probe of ultra-cold atoms by investigating Bragg scattering of a weakly attractive, Cooper paired, Fermi gas. Our calculations differ from existing theoretical treatments by: (i) providing explicit solutions for the time evolution of the matter field subjected to a moving optical grating, allowing direct observation of the dynamic response of the gas in momentum space, (ii) investigating in detail the large momentum transfer regime, where the atoms scatter well outside the Fermi sea, and, (iii) determining the Bragg spectrum of the Fermi gas in an analogous way to the case for a Bose-Einstein condensate [2, 11], by calculating the momentum transfer per atom over a range of Bragg detunings. The key result we report is Bragg scattering of correlated atom pairs via generation of a Bragg grating in the pair potential.

Our theoretical treatment is based on a mean-field description of a weakly interacting degenerate Fermi gas, where the collisional interaction Hamiltonian is approximated by a number of single-particle terms. Two spin states are present in equal numbers with field operators  $\hat{\psi}_{\uparrow}(\mathbf{r}, t)$  and  $\hat{\psi}_{\downarrow}(\mathbf{r}, t)$ , respectively. For convenience, the optical Bragg field is chosen so that it does not flip the particle spin. Implementing the Heisenberg equations of motion and the Bogoliubov transformation,

$$\hat{\psi}_{\uparrow,\downarrow}(\mathbf{r}, t) = \sum_{\mathbf{k}} \left[ u_{\mathbf{k}}(\mathbf{r}, t) \hat{\gamma}_{\mathbf{k}\uparrow,\mathbf{k}\downarrow} \mp v_{\mathbf{k}}^*(\mathbf{r}, t) \hat{\gamma}_{\mathbf{k}\downarrow,\mathbf{k}\uparrow}^\dagger \right], \quad (1)$$

yields [12, 13, 14] the time-dependent Bogoliubov de

Gennes equations,

$$i\hbar \frac{\partial}{\partial t} \begin{bmatrix} u_{\mathbf{k}}(\mathbf{r}, t) \\ v_{\mathbf{k}}(\mathbf{r}, t) \end{bmatrix} = \begin{bmatrix} L(\mathbf{r}, t) & \Delta(\mathbf{r}, t) \\ \Delta^*(\mathbf{r}, t) & -L(\mathbf{r}, t) \end{bmatrix} \begin{bmatrix} u_{\mathbf{k}}(\mathbf{r}, t) \\ v_{\mathbf{k}}(\mathbf{r}, t) \end{bmatrix}, \quad (2)$$

where

$$L(\mathbf{r}, t) = -\frac{\hbar^2 \nabla^2}{2M} + V_T(\mathbf{r}) + V_{\text{opt}}(\mathbf{r}, t) - E_F + U(\mathbf{r}, t). \quad (3)$$

The Hartree potential is  $U(\mathbf{r}, t) = V \langle \hat{\psi}_{\alpha}^\dagger(\mathbf{r}, t) \hat{\psi}_{\alpha}(\mathbf{r}, t) \rangle$ , the pair potential is  $\Delta(\mathbf{r}, t) = -V \langle \hat{\psi}_{\uparrow}(\mathbf{r}, t) \hat{\psi}_{\downarrow}(\mathbf{r}, t) \rangle$ , and  $u_{\mathbf{k}}(\mathbf{r}, t)$  and  $v_{\mathbf{k}}(\mathbf{r}, t)$  are the time-dependent *quasi-particle* amplitudes. We denote the Fermi energy by  $E_F = \hbar\omega_F = \hbar^2 k_F^2 / 2M$ , the atom mass by  $M$ , and the strength of the attractive collisional interaction between fermions by  $V$  ( $V < 0$ ). At  $t = 0$  the trapping potential  $V_T(\mathbf{r})$  is turned off, and the Bragg field  $V_{\text{opt}}(\mathbf{r}, t) = A \cos(\mathbf{q} \cdot \mathbf{r} - \omega t) / 2$  is turned on. The wave vector  $\mathbf{q}$  is aligned with the  $x$  axis, and we consider the regime of first order Bragg scattering, where  $\omega \sim \hbar q^2 / 2M$  (e.g., [15]).

Details of our numerical method are given elsewhere [14, 16]. Briefly, the system ground state is approximated by solving the time-independent form of Eq. (2) in the local density approximation. In order to avoid the ultra-violet divergence that arises when evaluating the self-consistent fields we invoke a momentum space cutoff. The evolution of the matter field is determined by solving Eq. (2) using a fourth order Runge-Kutta method [16]. We present two-dimensional calculations for a zero temperature homogeneous Fermi gas, and discuss the effects of either finite temperature or a harmonic trapping potential  $V_T(x) = m\omega_T^2 x^2 / 2$ , using one-dimensional calculations. Our results provide a basis for predicting the behaviour of a Bragg scattered three-dimensional Fermi gas.

Figure 1 (left-hand column) shows the momentum distribution of a Bragg scattered two-dimensional homogeneous Fermi gas at zero temperature. The number density at momentum  $\hbar\mathbf{k}$  is given by  $n(\mathbf{k}, t) \propto \langle \hat{\phi}_{\alpha}^\dagger(\mathbf{k}, t) \hat{\phi}_{\alpha}(\mathbf{k}, t) \rangle$ , where the proportionality constant is chosen such that  $\int n(\mathbf{k}, t) d\mathbf{k} = 1$ , and  $\hat{\phi}_{\alpha}(\mathbf{k}, t) =$

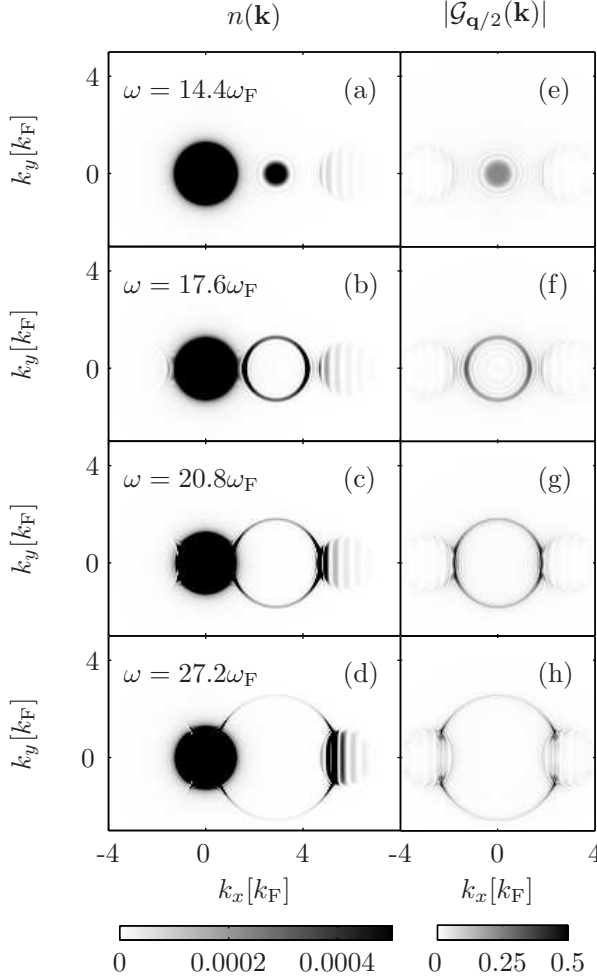


FIG. 1: Momentum distribution  $n(\mathbf{k})$ , and pair correlation function  $\mathcal{G}_{\mathbf{q}/2}(\mathbf{k})$ , of a Bragg scattered two-dimensional homogeneous Fermi gas at zero temperature. The momentum distribution of the initial cloud is saturated on the chosen scale in order to observe the scattered atoms ( $\approx 2\%$ ). Parameters are  $A = 1.80E_F$ ,  $q = 5.78k_F$ ,  $t = 8.22/\omega_F$ ,  $U = -0.169E_F$ ,  $\Delta = 0.203E_F$ , and (a), (e)  $\omega = 14.4\omega_F$ , (b), (f)  $\omega = 17.6\omega_F$ , (c), (g)  $\omega = 20.8\omega_F$ , and (d), (h)  $\omega = 27.2\omega_F$ .

$\int \hat{\psi}_\alpha(\mathbf{r}, t) \exp(-i\mathbf{k} \cdot \mathbf{r}) d\mathbf{r} / (L)^{d/2}$  is the field operator in momentum space, for a  $d$ -dimensional computational area of length  $L$ . The two spin states are scattered identically because of our choice of a spin preserving Bragg field. The initial cloud, centered at  $\mathbf{k} = \mathbf{0}$ , is scattered via two different mechanisms: (i) by single-particle scattering where an atom interacting with the optical Bragg field receives a momentum kick  $\hbar\mathbf{q}$ , and, (ii) by correlated-pair scattering, resulting in a ring of atoms centered at  $\mathbf{k} = \mathbf{q}/2$ . The atoms scattered into the ring are correlated about  $\mathbf{k} = \mathbf{q}/2$ , as demonstrated by the pair correlation function  $\mathcal{G}_{\mathbf{q}/2}(\mathbf{k}, t) = \langle \hat{\phi}_\uparrow(\mathbf{q}/2 + \mathbf{k}, t) \hat{\phi}_\downarrow(\mathbf{q}/2 - \mathbf{k}, t) \rangle$ , which is shown in Fig. 1 (right-hand column) [18]. Correlated-pair Bragg scattering is the main result of this paper, and is a signature of the initial Cooper paired state.

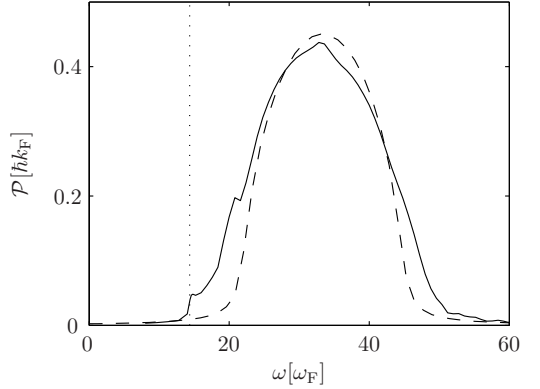


FIG. 2: Bragg spectrum of a two-dimensional homogeneous Fermi gas at zero temperature. Parameters are  $A = 1.80E_F$ ,  $q = 5.78k_F$ ,  $t = 8.22/\omega_F$ , and (dashed)  $U = 0E_F$ , and  $\Delta = 0E_F$ , and (solid)  $U = -0.169E_F$ , and  $\Delta = 0.203E_F$ . The vertical dotted line indicates  $\omega = \omega_{\text{thres}}$ .

We determine the Bragg spectrum of the degenerate Fermi gas by calculating the momentum transfer per atom along the Bragg axis,  $\mathcal{P}(t) = \int [\hbar\mathbf{k} \cdot \hat{\mathbf{q}}] n(\mathbf{k}, t) d\mathbf{k}$ , for a range of Bragg detunings. The Bragg spectrum of a two-dimensional homogeneous Fermi gas at zero temperature is given in Fig. 2. The spectrum has two main features resulting from the two different scattering mechanisms: (i) a broad resonance, also observed in the non-interacting case, due to single-particle scattering, and (ii) a low-frequency feature due to correlated-pair scattering (indicated by the vertical dotted line in Fig. 2).

Single-particle Bragg scattering is familiar from Bragg scattering of a Bose-Einstein condensate and is well understood theoretically (e.g., [15]). It is mediated directly by the optical grating and scatters atoms, via two-photon transitions, by momentum  $\hbar\mathbf{q}$ . In our calculations for a degenerate Fermi gas, single-particle scattering is accompanied by depletion of the pair potential  $\Delta(\mathbf{r}, t)$ , indicating that pairs are being broken. The resonance condition is well approximated using energy conservation arguments for non-interacting particles, i.e., by considering an atom scattered from momentum  $\hbar\mathbf{k}_R$  to  $\hbar(\mathbf{k}_R + \mathbf{q})$ . That gives the expression

$$\omega_{\text{sp}} = \frac{\hbar}{2M} (q^2 + 2\mathbf{k}_R \cdot \mathbf{q}), \quad (4)$$

which can be interpreted as specifying the initial momentum class that is scattered for given Bragg parameters. The broad resonance in the Bragg spectrum (see Fig. 2) is due to single-particle scattering and is centered at  $\omega = \hbar q^2 / 2M$ . The frequency width of the resonance is

$$\delta\omega \approx \frac{2\hbar q k'_F}{M} + \frac{A}{\hbar}, \quad (5)$$

where the first term accounts for the width of the initial momentum distribution, and the second term is due to

power broadening (e.g., [15]). We have defined a modified Fermi momentum by  $\hbar^2 k_F'^2/2M = E_F - U$  (e.g., [17]).

Bragg scattering of correlated atom pairs gives rise to a ring of atoms centered at momentum  $\hbar\mathbf{q}/2$  (see Fig. 1), and increased momentum transfer at low frequencies (see Fig. 2). The atoms that form the ring come primarily from the Fermi surface and are not the result of direct Bragg scattering from the optical grating, which scatters atoms by integer multiples of the Bragg momentum  $\hbar\mathbf{q}$ . Correlated-pair scattering is associated with formation of a moving grating in the pair potential, that is well approximated by  $\Delta(\mathbf{r}, t) \approx \Delta_0(t) + \Delta_1(t) \exp[i(\mathbf{q} \cdot \mathbf{r} - \omega t)]$ . The Bragg grating in the pair potential scatters Cooper pairs (of zero centre-of-mass momentum) to centre-of-mass momentum  $\hbar\mathbf{q}$ . The individual momenta of the two atoms are  $\hbar(\mathbf{q}/2 \pm \mathbf{k}_{\text{rel}})$ , and the scattered atoms retain their pairing (see Fig. 1). A resonance condition for correlated-pair Bragg scattering can be obtained from energy conservation arguments to be

$$\omega_{\text{pair}} = \frac{\hbar}{M} \left( \frac{q^2}{4} + k_{\text{rel}}^2 \right) - \frac{\hbar k_F'^2}{M}. \quad (6)$$

Below the threshold detuning  $\omega_{\text{thres}} = \hbar q^2/4M - \hbar k_F'^2/M$ , the pair potential grating does not provide sufficient energy for pairs to be scattered. At the threshold, [see Fig. 1(a)], both atoms of a scattered pair have the same momentum  $\hbar\mathbf{q}/2$ . Above the threshold, excess energy provided by the pair potential grating is distributed equally between the two atoms of the scattered pair, each atom carrying additional kinetic energy  $\hbar^2 k_{\text{rel}}^2/2M$ .

We can understand some important features of Bragg scattering of correlated pairs with an approximate analytic treatment in the homogeneous case at zero temperature. Neglecting the trapping potential [ $V_T(\mathbf{r}) = 0$ ], the periodicity of the Bragg field leads to solutions of Eq. (2) that have the Bloch form, and can be expanded as

$$\begin{aligned} u_{\mathbf{k}}(\mathbf{r}, t) &= e^{i\mathbf{k} \cdot \mathbf{r}} \sum_n a_n^{\mathbf{k}}(t) e^{in(\mathbf{q} \cdot \mathbf{r} - \omega t)} \\ v_{\mathbf{k}}(\mathbf{r}, t) &= e^{i\mathbf{k} \cdot \mathbf{r}} \sum_n b_n^{\mathbf{k}}(t) e^{in(\mathbf{q} \cdot \mathbf{r} - \omega t)}, \end{aligned} \quad (7)$$

where  $n$  is an integer. The self-consistent potentials are periodic, with the translational symmetry of the Bragg field, i.e.,

$$\begin{aligned} U(\mathbf{r}, t) &= \sum_n U_n(t) e^{in(\mathbf{q} \cdot \mathbf{r} - \omega t)} \\ \Delta(\mathbf{r}, t) &= \sum_n \Delta_n(t) e^{in(\mathbf{q} \cdot \mathbf{r} - \omega t)}. \end{aligned} \quad (8)$$

Evolution equations for the coefficients  $a_n^{\mathbf{k}}(t)$  and  $b_n^{\mathbf{k}}(t)$  can be derived from Eq. (2) to be

$$\begin{aligned} i\hbar \frac{da_n^{\mathbf{k}}(t)}{dt} &= \hbar\omega_n^a(\mathbf{k}) a_n^{\mathbf{k}}(t) + \frac{A}{4} [a_{n+1}^{\mathbf{k}}(t) + a_{n-1}^{\mathbf{k}}(t)] \\ &+ \sum_m U_m(t) a_{n-m}^{\mathbf{k}}(t) + \sum_m \Delta_m(t) b_{n-m}^{\mathbf{k}}(t), \end{aligned} \quad (9)$$

and

$$\begin{aligned} i\hbar \frac{db_n^{\mathbf{k}}(t)}{dt} &= \hbar\omega_n^b(\mathbf{k}) b_n^{\mathbf{k}}(t) - \frac{A}{4} [b_{n+1}^{\mathbf{k}}(t) + b_{n-1}^{\mathbf{k}}(t)] \\ &- \sum_m U_m(t) b_{n-m}^{\mathbf{k}}(t) + \sum_m \Delta_m^*(t) a_{n+m}^{\mathbf{k}}(t), \end{aligned} \quad (10)$$

where  $\hbar\omega_n^{a,b}(\mathbf{k}) = \pm [\hbar^2(\mathbf{k} + n\mathbf{q})^2/2M - E_F] - n\hbar\omega$ . Initially the only non-zero coefficients are  $a_0^{\mathbf{k}}$  (for  $|\mathbf{k}| \gtrsim k_F'$ ) and  $b_0^{\mathbf{k}}$  (for  $|\mathbf{k}| \lesssim k_F'$ ). The mean-field coefficients  $U_m(t)$  and  $\Delta_m(t)$  must be obtained self-consistently, in particular

$$\Delta_m(t) = -V \sum_{\mathbf{k}} \sum_n a_n^{\mathbf{k}}(t) b_{n-m}^{\mathbf{k}*}(t). \quad (11)$$

First order correlated-pair Bragg scattering is mediated by a moving grating in the pair potential, arising due to the terms  $m = 1, n = 0, 1$  in Eq. (11) becoming non-zero. The grating forms for frequencies at and above  $\omega_{\text{thres}}$ , which is on the low frequency edge of the single-particle Bragg resonance (see Fig. 2). The pair potential grating is seeded by red-detuned single-particle Bragg scattering from the Fermi surface, i.e., in the region  $\mathbf{k}_R \approx -k_F' \hat{\mathbf{x}}$ . In the seeding process a paired atom from momentum  $\hbar\mathbf{k}_R$  is scattered to  $\hbar(\mathbf{k}_R + \mathbf{q})$ , but the process is so far detuned that the scattered atom retains some part of its correlation with its paired atom, at momentum  $-\hbar\mathbf{k}_R \approx \hbar k_F' \hat{\mathbf{x}}$ . It can be shown, from Eqs. (9) and (10), that red-detuned single-particle transitions contribute to the formation of  $\Delta_1(t)$  by generating coefficients  $a_1^{\mathbf{k}}(t)$  and  $b_{-1}^{\mathbf{k}}(t)$  (primarily in the region  $|\mathbf{k}| \approx k_F'$ ), thus generating non-zero contributions  $a_1^{\mathbf{k}}(t) b_0^{\mathbf{k}*}(t)$  and  $a_0^{\mathbf{k}}(t) b_{-1}^{\mathbf{k}*}(t)$ . The process of seeding the pair potential grating can be observed in the left-hand column of Fig. 1, where a fraction of the left-hand edge of the Fermi surface is scattered by momentum  $\hbar\mathbf{q}$ .

Following the initiation of the pair potential grating, its subsequent development can be understood in terms of a truncated version of Eqs. (9) and (10), i.e.,

$$i\hbar \frac{d}{dt} \begin{bmatrix} a_0^{\mathbf{k}}(t) \\ b_{-1}^{\mathbf{k}}(t) \end{bmatrix} = \begin{bmatrix} \epsilon_0^a(\mathbf{k}) & \Delta_1(t) \\ \Delta_1^*(t) & \epsilon_{-1}^b(\mathbf{k}) \end{bmatrix} \begin{bmatrix} a_0^{\mathbf{k}}(t) \\ b_{-1}^{\mathbf{k}}(t) \end{bmatrix}, \quad (12)$$

which is appropriate for describing the scattered pairs ( $|\mathbf{k}| > k_F'$ ). In Eq. (12),  $\epsilon_n^{a,b}(\mathbf{k}) = \hbar\omega_n^{a,b}(\mathbf{k}) \pm U_0$ , and  $\Delta_1(t) = -V \sum_{\mathbf{k}} a_0^{\mathbf{k}}(t) b_{-1}^{\mathbf{k}*}(t)$ , where  $a_0^{\mathbf{k}}(t) b_{-1}^{\mathbf{k}*}(t)$  only becomes significant if  $\epsilon = \epsilon_0^a(\mathbf{k}) - \epsilon_{-1}^b(\mathbf{k}) \approx 0$ . The behaviour of  $\Delta_1(t)$  depends markedly on the choice of the Bragg parameters  $\omega$  and  $\mathbf{q}$ . However, a regime exists where  $\Delta_1(t)$  grows significantly, due to the scattered pairs. That regime can be found from Eq. (12) by assuming a self-consistent  $\Delta_1(t)$  varying slowly with time. In that case, an approximate solution for  $a_0^{\mathbf{k}}(t) b_{-1}^{\mathbf{k}*}(t)$  is

$$a_0^{\mathbf{k}}(t) b_{-1}^{\mathbf{k}*}(t) = \frac{\Delta_1 |a_0^{\mathbf{k}}(0)|^2}{\hbar^2 \Omega^2} [\epsilon(1 - \cos \Omega t) + i\hbar\Omega \sin \Omega t], \quad (13)$$

where  $\hbar^2\Omega^2 = \epsilon^2 + 4|\Delta_1|^2$ . With solution (13), the summand in  $\Delta_1(t)$  has a point of stationary phase at  $\mathbf{k} = \mathbf{q}/2$ , i.e., at the threshold frequency  $\omega_{\text{thres}}$ . At that point  $\epsilon = 0$  and from Eq. (13) we see that terms with  $\mathbf{k} \approx \mathbf{q}/2$  grow steadily [ $\sim \sin(2|\Delta_1|t/\hbar)$ ] over the duration of the Bragg pulse. Thus, we have a self-consistent solution, one that is confirmed by our numerical calculations. Growth of  $\Delta_1(t)$  at the threshold frequency enhances population transfer to momentum  $\hbar\mathbf{q}/2$ .

Correlated-pair scattering can also conserve energy ( $\epsilon = 0$ ) for  $\omega > \omega_{\text{thres}}$  [see Fig. 1(b)-(d)]. Above threshold the atoms scatter to momenta  $\hbar(\mathbf{q}/2 \pm \mathbf{k}_{\text{rel}})$ , where  $\omega - \omega_{\text{thres}} = \hbar k_{\text{rel}}^2/M$ . The terms (13) have no stationary phase about momentum  $\hbar\mathbf{k}_{\text{rel}}$ , so above threshold  $\Delta_1(t)$  is not strongly enhanced by the scattered pairs. On the other hand, the momentum space region occupied by the scattered pairs is larger above threshold, compared to at threshold. The thickness  $\delta k$  of the ring can be estimated by assuming a frequency width  $\Gamma$ , determined by the Bragg pulse length ( $\Gamma \approx \pi/t$ ), and setting  $\delta\epsilon = \hbar\Gamma$ , to find that

$$\delta k \approx \sqrt{\frac{\pi M}{\hbar t} + k_{\text{rel}}^2} - k_{\text{rel}}. \quad (14)$$

In two dimensions  $\delta k \sim k_{\text{rel}}^{-1}$ , for large  $k_{\text{rel}}$ , and the momentum space area over which the ring is populated is constant with  $k_{\text{rel}}$ . In three dimensions the volume of the momentum space spherical shell occupied by the scattered pairs increases linearly with  $k_{\text{rel}}$ .

We have investigated the dependence of the correlated-pair scattering on a range of system parameters. By increasing the initial pairing in the system (increasing  $|V|$ ), we find in our treatment that the number of correlated pairs scattered increases. However, the validity of the mean-field approach is questionable when  $|V|$  becomes too large. The number of correlated pairs scattered can also be increased by enhancing the single-particle scattering processes that seed the pair potential grating, either by increasing the Bragg field strength  $A$ , or by reducing the Bragg wave vector  $\mathbf{q}$  (to make the seeding more resonant).

Investigating the effect of finite temperature, or inhomogenous systems (i.e., initially trapped systems), is computationally intensive. For those cases we have calculated numerical solutions to Eq. (2) with one spatial dimension. We find that in one dimension the correlated-pair scattering feature in the Bragg spectrum is a pronounced narrow peak at the threshold frequency  $\omega_{\text{thres}}$ . As expected, the pair potential grating is enhanced at threshold, but above threshold the total number of scattered correlated pairs decreases rapidly because the momentum space region available for the scattered pairs is small in one dimension. The effect of finite temperature is to reduce the initial pairing in the system and, therefore, to reduce the number of scattered pairs accordingly. For an initially trapped Fermi gas, the self-consistent fields,

and in particular  $\Delta(\mathbf{r}, t)$ , have an initial spatial dependence, meaning that the threshold frequency is not the same for all pairs. While correlated scattering still occurs, there are a range of possible  $\mathbf{k}_{\text{rel}}$  values and the scattered ring becomes filled in.

In conclusion, our numerical solutions of the time-dependent Bogoliubov de Gennes equations show that Bragg scattering of a Fermi gas, with a momentum transfer well outside the Fermi surface, gives rise to Bragg scattering of correlated atom pairs. At low frequencies, correlated-pair scattering dominates the more familiar single-particle Bragg scattering, and has a distinctive signature in momentum space, namely a ring structure (in two dimensions) or a spherical shell (in three dimensions) centered at half the usual Bragg momentum transfer. The correlated-pair scattering arises from a Bragg grating formed in the pair potential, and it has a sharp frequency threshold. We have developed an analytic model that explains the mechanism by which the grating is generated, and provides quantitative predictions of a number of key features of the correlated scattering. In this paper detailed numerical results have been given for a zero temperature homogeneous two-dimensional system, and our analytic model shows that correlated-pair scattering will occur in three dimensions. We have also shown using one-dimensional calculations that the phenomenon is robust to the effects of finite temperature and spatial inhomogeneity.

This work was supported by Marsden Fund UOO0509 and the Tertiary Education Commission (TAD 884).

---

\* Electronic address: kchallis@physics.otago.ac.nz

- [1] M. Kozuma, L. Deng, E. W. Hagley, J. Wen, R. Lutwak, K. Helmerson, S. L. Rolston, and W. D. Phillips, *Phys. Rev. Lett.* **82**, 871 (1999).
- [2] D. M. Stamper-Kurn, A. P. Chikkatur, A. Görlitz, S. Inouye, S. Gupta, D. E. Pritchard, and W. Ketterle, *Phys. Rev. Lett.* **83**, 2876 (1999).
- [3] S. Richard, F. Gerbier, J. H. Thywissen, M. Hugbart, P. Bouyer, and A. Aspect, *Phys. Rev. Lett.* **91**, 010405 (2003).
- [4] P. B. Blakie and R. J. Ballagh, *Phys. Rev. Lett.* **86**, 3930 (2001).
- [5] R. Geursen, N. R. Thomas, and A. C. Wilson, *Phys. Rev. A* **68**, 043611 (2003).
- [6] K. J. Challis and R. J. Ballagh, *Phys. Rev. A* **71**, 033620 (2005).
- [7] J. Ruostekoski, *Phys. Rev. A* **60**, R1775 (1999).
- [8] M. Rodriguez and P. Törmä, *Phys. Rev. A* **66**, 033601 (2002).
- [9] H. P. Büchler, P. Zoller, and W. Zwerger, *Phys. Rev. Lett.* **93**, 080401 (2004).
- [10] Bimalendu Deb, *J. Phys. B* **39**, 529 (2006).
- [11] P. B. Blakie, R. J. Ballagh, and C. W. Gardiner, *Phys. Rev. A* **65**, 033602 (2002).
- [12] P. G. de Gennes, *Superconductivity of metals and alloys*

- (W. A. Benjamin, Inc., New York, 1966).
- [13] J. B. Ketterson and S. N. Song, *Superconductivity* (Cambridge University Press, Cambridge, 1999).
- [14] K. J. Challis, R. J. Ballagh, and C. W. Gardiner, in preparation.
- [15] P. B. Blakie and R. J. Ballagh, *J. Phys. B* **33**, 3961 (2000).
- [16] R. J. Ballagh, *Computational methods for nonlinear partial differential equations*, <http://www.physics.otago.ac.nz> (2000).
- [17] N. Nygaard, G. M. Bruun, C. W. Clark, and D. L. Feder, *Phys. Rev. Lett.* **90**, 210402 (2003).
- [18] The maximum possible correlation for a pair of atoms with momenta  $\pm\hbar\mathbf{k}$  is  $|\mathcal{G}_0(\mathbf{k}, t)| = 1/2$ .